Schweizerische Eidgenossenschaft
Confédération suisse
Confederazione Svizzera
Confederaziun svizra

Swiss Confederation

Federal Department of Home Affairs FDHA
Federal Office of Meteorology and Climatology MeteoSwiss

Photographic Visualization of Weather Forecasts with Generative Adversarial Networks

ECMWF Machine Learning Workshop
March 31st, 2022

Christian Sigg (MeteoSwiss), Flavia Cavallaro (Comerge),
Tobias Günther (FAU) and Martin R. Oswald (ETH Zürich and UvA)

Contact: christian.sigg@meteoswiss.ch

Outline

- Motivation: Why Photographic Images?
- Baseline and Evaluation Criteria
- Method: Conditional GANs
- Results
- Conclusions and Future Work

Outdoor Weather Cameras

An information-dense yet accessible visualization of past and present weather:

Visualization of Weather Forecasts

Screenshots of the MeteoSwiss smartphone app

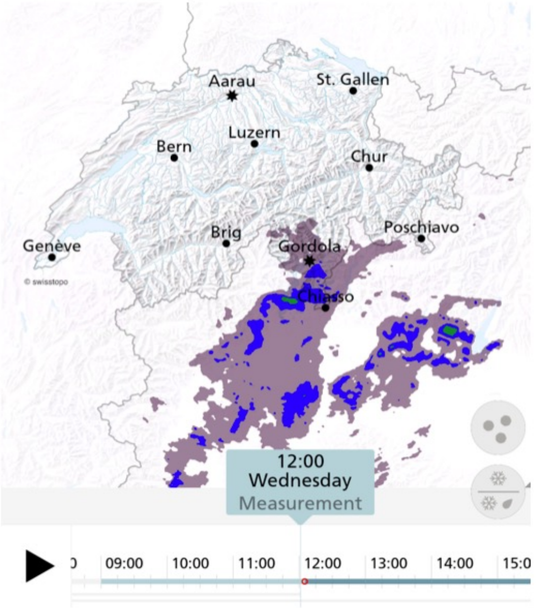

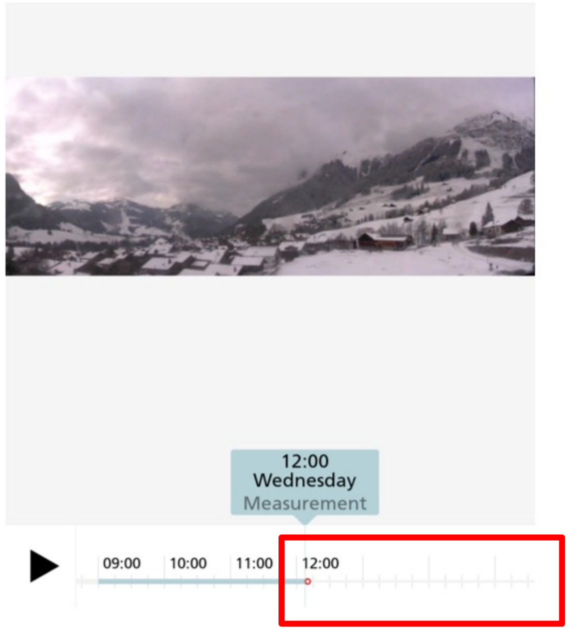

observation *forecast* *observation* *forecast* *observation*

Also use photographic images to visualize future weather conditions!

Outline

- Motivation: Why Photographic Images?
- Baseline and Evaluation Criteria
- Method: Conditional GANs
- Results
- Conclusions and Future Work

Baseline: Analog Retrieval

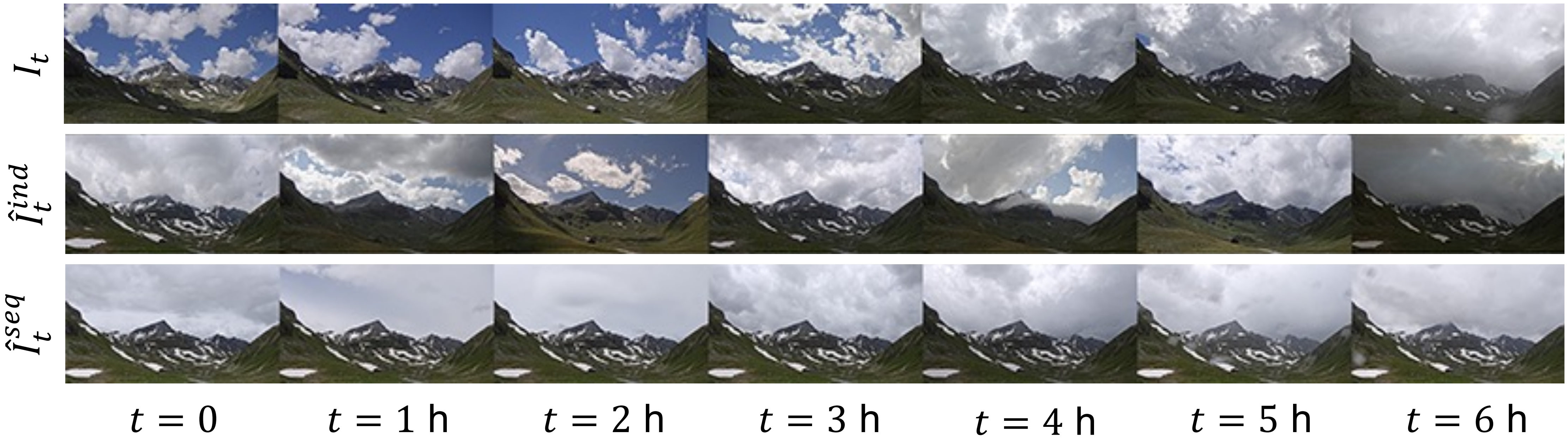

I_t Image sequence taken at Flüela, 10 to 16 UTC on July 2nd, 2020

$\hat{I}_t^{ind}$ Retrieval of best matching individual images from annotated archive

$\hat{I}_t^{seq}$ Retrieval of best matching sequence

Proposed Evaluation Criteria

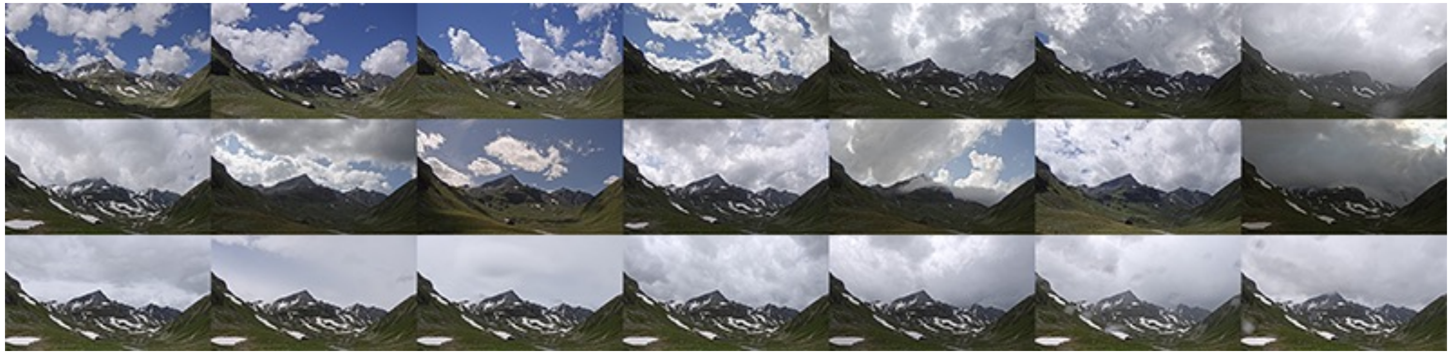

I. Images should look real, no obvious artifacts
II. Match future atmospheric, ground and illumination conditions
III. Seamless transition from observation to forecast
IV. Visual continuity between consecutive images

Evaluation of Analog Retrieval

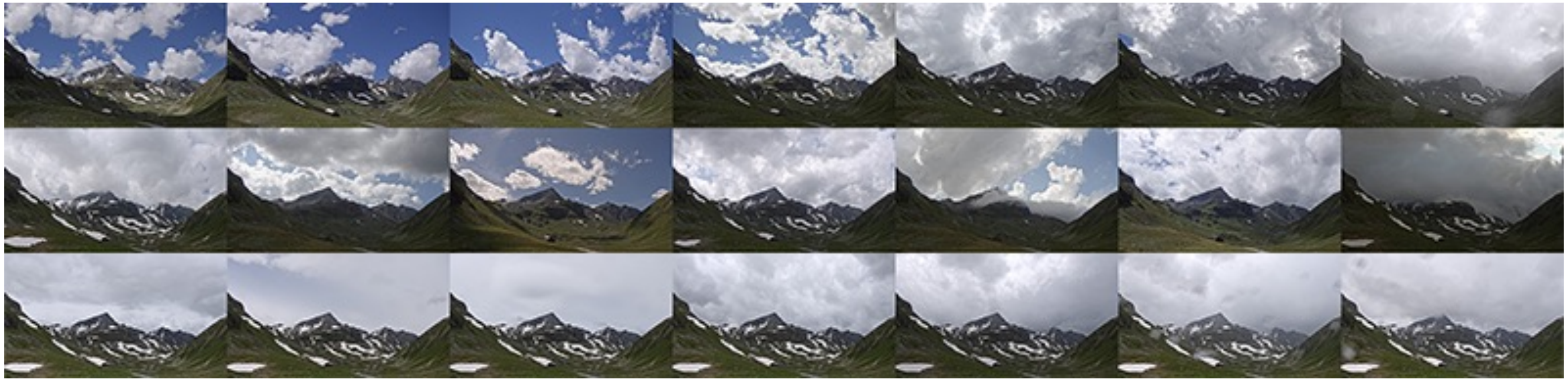

observations

analog images

analog sequence

	I. Realism	II. Matching conditions	III. Seamless transition	IV. Visual continuity
Analog images	🙂	😐	🙁	🙁
Analog sequence	🙂	🙁	🙁	🙂

High information density of images → retrieving analogs is not feasible 🤔

Outline

- Motivation: Why Photographic Images?
- Baseline and Evaluation Criteria
- Method: Conditional GANs
- Results
- Conclusions and Future Work

Image Synthesis: A Regression Problem

Generate photographic image $\hat{I}_t$, given forecast w_t of future weather conditions

$$G: w_t \mapsto \hat{I}_t$$

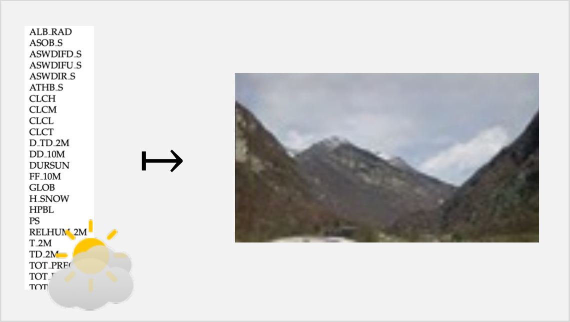

Generator $G(w;\theta)$ is a neural network, θ trained by minimizing expected loss

$$\operatorname{argmin}_\theta \mathbb{E}_{w_t, I_t}[L(G(w;\theta), I_t)]$$

Choice of Loss Function L

$$\text{argmin}_\theta \; \mathbb{E}_{w_t, I_t}[L(G(w_t; \theta), I_t)]$$

Forecast w_t does not determine exact shapes and locations of clouds
→ Pixel-wise loss function is not appropriate, results in uniform sky:

$\hat{I}_t$ for L_1 loss

I_t

Goal: User should not be able to tell whether I_t or $\hat{I}_t$ is the real image, even if they are not identical.

Generative Adversarial Networks Goodfellow et al., 2014

Discriminator $D: I \mapsto [0, 1]$ mimics user, learns loss function through adversarial training

Generator $G: z \mapsto I$, creates image I from random input $z \sim \mathcal{N}(0, 1)$

$$\min_\theta \max_\eta \mathbb{E}_I[\log D(I; \eta)] + \mathbb{E}_z[\log\{1 - D(G(z; \theta); \eta\}]$$

authenticate real images

fool discriminator

spot fake images

Generator Architecture

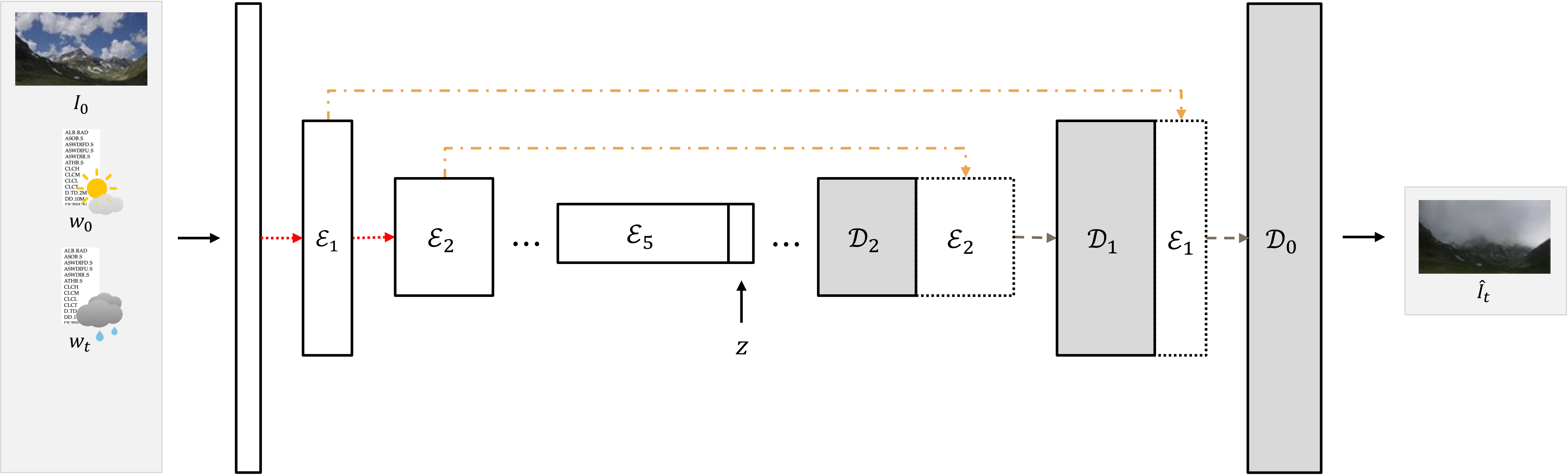

- Conditional Generator Mirza and Osindero, 2014 transforms current image I_0
- Encoder-decoder with skip connections Ronneberger et al., 2015
- Spectral normalization applied to all convolution layers Miyato et al., 2018

Discriminator Architecture

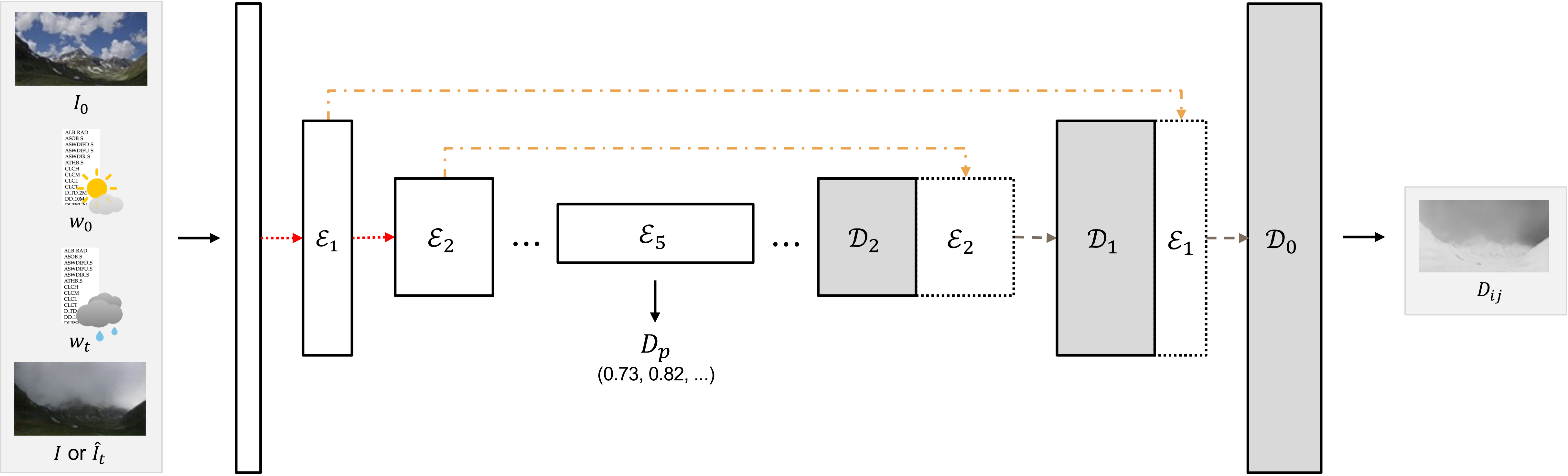

- Conditional discriminator $D(I|I_0, w_0, w_t)$
- Two output heads: patch-level D_p and pixel-l D_{ij} Schonfeld et al., 2020

Outline

Evaluation Data

Cevio (elevation 421 m)

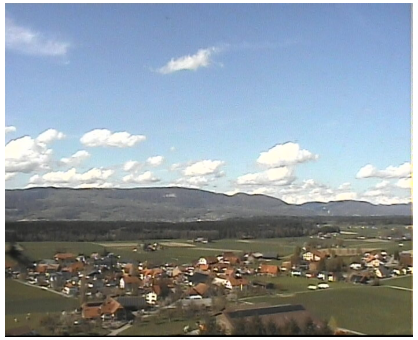

Etziken (elevation 524 m)

Flüela (elevation 2177 m)

Descriptor w: time of day, day of year, 31 COSMO-1 hourly output fields

Training: all pairs (I_0, w_0) and (I_t, w_t), $t \in [0, 10, 20, \ldots, 360\ \mathrm{min}]$ of 2019

Test: Jan to Aug of year 2020 (until decommissioning of COSMO-1 at MCH)

Downscaled to 64 x 128 pixels to speed up training and conserve GPU memory

I. Realism

What is your first impression of the image?

generated

real

generated

real

I. Realism

Results of study with 5 professional users of MCH camera feeds:

	Judgment	
Actual	Real	Generated
Real	57	18
Generated	43	32

Cevio: 59 % accuracy

	Judgment	
Actual	Real	Generated
Real	52	23
Generated	32	43

Etziken: 63 % accuracy

	Judgment	
Actual	Real	Generated
Real	57	18
Generated	49	26

Flüela: 55 % accuracy

User accuracy is not much better than random guessing 🙂

II. Matching Weather Conditions

Atmosphere: cloud cover, cloud type, visibility

Ground: dry, wet, frost, snow

Illumination: time of day, diffuse or direct

II. Matching Weather Conditions

	Matching conditions					
	Atmosphere				Illumination	
Camera	Cloud cover	Cloud type	Visibility	Ground	Time of day	Diffuse/direct
Cevio	32	35	45	45	45	40
Etziken	36	36	44	45	45	38
Flüela	31	33	26	44	41	35

Example: Mismatch in cloud cover

$\hat{I}_t$

I_t

but forecast w_t predicted 100 % cloud area fraction in medium troposphere

II. Matching Weather Conditions

	Matching conditions						
	Atmosphere				Illumination		
Camera	Cloud cover	Cloud type	Visibility	Ground	Time of day	Diffuse/direct	Viz. failures
Cevio	32	35	45	45	45	40	5
Etziken	36	36	44	45	45	38	2 🙂
Flüela	31	33	26	44	41	35	5

Visualization failure: forecast w_t is accurate, but generated image $\hat{I}_t$ is inconsistent with it

III. Seamless Transition – IV. Visual Continuity

I_t

$\hat{I}_t$

$t = 0$ $t = 1$ h $t = 2$ h $t = 3$ h $t = 4$ h $t = 5$ h $t = 6$ h

Possible because G is conditioned on I_0, compare to analog retrieval:

$\hat{I}_t^{ind}$

$\hat{I}_t^{seq}$

Outline

- Motivation: Why Photographic Images?
- Baseline and Evaluation Criteria
- Method: Conditional GANs
- Results
- Conclusions and Future Work

Conclusions

- Photographic images can also visualize future weather conditions
- Look realistic, match predicted weather conditions, attain seamless transition from observation to forecast and visual continuity

Applications:

- Communicate localized forecasts in webcam feeds, smartphone app
- Provide similar service to communities and tourism organizations

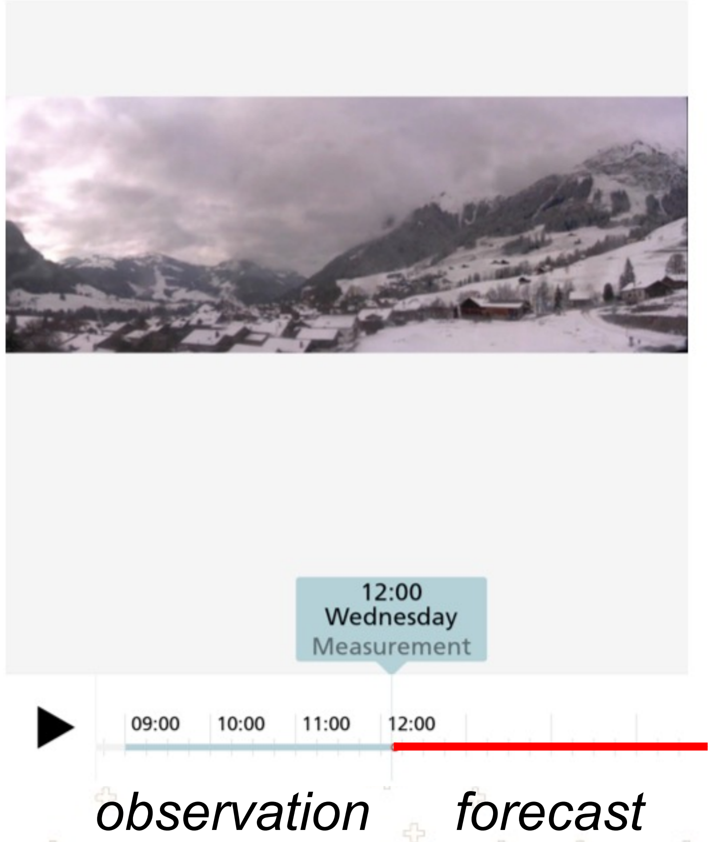

Future Work

- Use more accurate and descriptive weather descriptors
- Scale image size beyond 64 x 128 pixels e.g. Karras et al., 2018
- Improve transformations involving translations:

I_t

$\hat{I}_t$

$t = 0$ $t = 1$ h $t = 2$ h $t = 3$ h $t = 4$ h $t = 5$ h $t = 6$ h

(including self-attention layers Zhang et al., 2019 did not help)

- Synthesize whole sequences to improve temporal evolution Wu et al., 2020

Resources

The pre-print of our paper is available at

https://arxiv.org/abs/2203.15601

Tensorflow code, trained models and results are available at

https://github.com/meteoswiss/photocast

Acknowledgments

We thank Rega for giving us the permission to use images from the Cevio camera in this study.

We thank Tanja Weusthoff for the preparation of the COSMO-1 forecast data.

We thank Christian Allemann, Yannick Bernard, Eliane Thürig, Deborah van Geijtenbeek and Abbès Zerdouk for evaluating the realism of individual generated images.

We thank Daniele Nerini for providing his expertise on nowcasting and post-processing of forecasts.

Bibliography

Goodfellow, I., Pouget-Abadie, J., Mirza, M., Xu, B., Warde-Farley, D., Ozair, S., ... & Bengio, Y. (2014). Generative adversarial nets. Advances in neural information processing systems, 27.

He, K., Zhang, X., Ren, S., & Sun, J. (2016). Deep residual learning for image recognition. In Proceedings of the IEEE conference on computer vision and pattern recognition (pp. 770-778).

Karras, T., Aila, T., Laine, S., & Lehtinen, J. (2017). Progressive growing of gans for improved quality, stability, and variation. arXiv preprint arXiv:1710.10196.

Mirza, M., & Osindero, S. (2014). Conditional generative adversarial nets. arXiv preprint arXiv:1411.1784.

Miyato, T., Kataoka, T., Koyama, M., & Yoshida, Y. (2018). Spectral normalization for generative adversarial networks. arXiv preprint arXiv:1802.05957.

Ronneberger, O., Fischer, P., & Brox, T. (2015, October). U-net: Convolutional networks for biomedical image segmentation. In International Conference on Medical image computing and computer-assisted intervention (pp. 234-241).

U. Schättler, G. Doms, and C. Schraff. (2021). COSMO-Model Version 6.00: A Description of the Non- hydrostatic Regional COSMO-Model - Part VI: Model Output and Data Formats for I/O.

Schonfeld, E., Schiele, B., & Khoreva, A. (2020). A u-net based discriminator for generative adversarial networks. In Proceedings of the IEEE/CVF Conference on Computer Vision and Pattern Recognition (pp. 8207-8216).

Wu, S., Xiao, X., Ding, Q., Zhao, P., Wei, Y., & Huang, J. (2020). Adversarial sparse transformer for time series forecasting. Advances in Neural Information Processing Systems, 33, 17105-17115.

Yun, S., Han, D., Oh, S. J., Chun, S., Choe, J., & Yoo, Y. (2019). Cutmix: Regularization strategy to train strong classifiers with localizable features. In Proceedings of the IEEE/CVF international conference on computer vision (pp. 6023-6032).

Zhang, H., Goodfellow, I., Metaxas, D., & Odena, A. (2019, May). Self-attention generative adversarial networks. In International conference on machine learning (pp. 7354-7363). PMLR.

Generator Objectives to be Minimized

How much $G(I_0, z|w_0, w_t)$ struggles to fool the discriminator on the patch level

$$\mathbb{E}_{I_0,w_0,w_t}\mathbb{E}_z\left[\sum_p \log\left[D_p(G(I_0, z|w_0, w_t)|I_0, w_0, w_t)\right]\right]$$

and on the pixel level

$$\mathbb{E}_{I_0,w_0,w_t}\mathbb{E}_z\left[\sum_{ij} \log\left[D_{ij}(G(I_0, z|w_0, w_t)|I_0, w_0, w_t)\right]\right]$$

How similar two generated images look at the pixel level, given different random inputs $z_1, z_2 \sim \mathcal{N}(0,1)$

$$-\mathbb{E}_{I_0,w_0,w_t}\mathbb{E}_{z_1,z_2}\left[\sum_{ijc}\left|G_{ijc}(I_0, z_1|w_0, w_t) - G_{ijc}(I_0, z_2|w_0, w_t)\right|\right]$$

Discriminator Objectives to be Maximized

How well the patch head D_p authenticates real images

$$\mathbb{E}_{I_0,w_0,I_t w_t}\left[\sum_p \log D_p(I_t|I_0,w_0,w_t)\right]$$

and spots generated images

$$\mathbb{E}_{I_0,w_0,w_t}\mathbb{E}_z\left[\sum_p \log\left[1-D_p(G(I_0,z|w_0,w_t)|I_0,w_0,w_t)\right]\right]$$

How well the pixel head D_{ij} can distinguish pixels of a cut-mix Yun et al., 2019 composite C

$$\mathbb{E}_C\left[\sum_{ij} M_{ij}D_{ij}(C)+\left(1-M_{ij}\right)\log(1-D_{ij}(C))\right]$$

Artifacts Induced by Residual Learning He et al., 2015

Present image I_0

Forecast visualization $\hat{I}_t$

Clouds in I_0 are still partially visible in the clear sky regions of $\hat{I}_t$

→ Residual transformation learned by the generator does not fully cancel their appearance

Subset of COSMO-1 Output Fields Schättler et al., 2021

Abbreviation	Unit	Name
ALB_RAD	%	Surface albedo for visible range, diffuse
ASOB_S	W/m^2	Net short-wave radiation flux at surface
ASWDIFD_S	W/m^2	Diffuse downward short-wave radiation at the surface
ASWDIFU_S	W/m^2	Diffuse upward short-wave radiation at the surface
ASWDIR_S	W/m^2	Direct downward short-wave radiation at the surface
ATHB_S	W/m^2	Net long-wave radiation flux at surface
CLCH	%	Cloud area fraction in high troposphere (pressure below ca. 400 hPa)
CLCM	%	Cloud area fraction in medium troposphere (between ca. 400 and 800 hPa)
CLCL	%	Cloud area fraction in low troposphere (pressure above ca. 800 hPa)
CLCT	%	Total cloud area fraction
D_TD_2M	K	2 m dew point depression
DD_10M	°	10 m wind direction
DURSUN	s	Duration of sunshine
FF_10M	m/s	10 m wind speed
GLOB	W/m^2	Downward shortwave radiation flux at surface
H_SNOW	m	Snow depth
HPBL	m	Height of the planetary boundary layer
PS	Pa	Surface pressure (not reduced)
RELHUM_2M	%	2 m relative humidity (with respect to water)
T_2M	K	2 m air temperature
TD_2M	K	2 m dew point temperature
TOT_PREC	kg/m^2	Total precipitation
TOT_RAIN	kg/m^2	Total precipitation in rain
TOT_SNOW	kg/m^2	Total precipitation in snow
U_10M	m/s	10 m grid eastward wind
V_10M	m/s	10 m grid northward wind
VMAX_10M	m/s	Maximum 10 m wind speed